

Local forest structure variability increases resilience to wildfire in dry western U.S. coniferous forests

Michael J. Koontz^{1,2,3*}, Malcolm P. North^{2,4}, Chhaya M. Werner^{2,5,6}, Stephen E. Fick^{7,8}, Andrew M. Latimer²

¹Graduate Group in Ecology, University of California; Davis, CA, USA

²Department of Plant Sciences, University of California; Davis, CA, USA

³Earth Lab, University of Colorado-Boulder; Boulder, CO, USA

⁴Pacific Southwest Research Station, USDA Forest Service; Mammoth Lakes, CA, USA

⁵Center for Population Biology, University of California; Davis, CA, USA

⁶German Centre for Integrative Biodiversity Research; Halle-Jena-Leipzig, Germany

⁷US Geological Survey, Southwest Biological Science Center

⁸Department of Ecology and Evolutionary Biology, University of Colorado; Boulder, CO, USA

*Correspondence: 4001 Discovery Drive; Boulder, CO 80303; michael.koontz@colorado.edu; (970) 682-4727

Coauthor emails: mnorth@ucdavis.edu (MPN), cwerner@ucdavis.edu (CMW), stephen.fick@gmail.com (SEF), amlatimer@ucdavis.edu (AML)

Running title: Remote sensing resistance

Keywords: resilience, wildfire, severity, texture analysis, forest structure, Sierra Nevada, forest, disturbance

Type of article: Letters

Abstract word count: 148

Main text word count: 4994 (Intro: 1176; Methods: 1509; Results: 482; Discussion: 1827)

Text boxes word count: 0

Number of... references: 111, figures: 5, tables: 1, text boxes: 0

Statement of authorship: MJK, CMW, SEF, MPN, and AML conceived the study. MJK, SEF, and CMW wrote the Earth Engine code. MJK performed the analysis, with input from all authors. MJK wrote the first draft of the manuscript. All authors contributed substantially to editing and revisions.

Data accessibility statement: The data and analysis code supporting the results are archived on the Open Science Framework at www.doi.org/10.17605/OSF.IO/27NSR.

Date report generated: October 21, 2019

28 **Abstract**

29 A “resilient” forest endures disturbance and is likely to persist. Resilience to wildfire may arise from feedback
30 between fire behavior and forest structure in dry forest systems. Frequent fire creates fine-scale variability in
31 forest structure, which may then interrupt fuel continuity and prevent future fires from killing overstory trees.
32 Testing the generality and scale of this phenomenon is challenging for vast, long-lived forest ecosystems. We
33 quantify forest structural variability and fire severity across >30 years and >1,000 wildfires in California’s
34 Sierra Nevada. We find that greater variability in forest structure increases resilience by reducing rates
35 of fire-induced tree mortality and that the scale of this effect is local, manifesting at the smallest spatial
36 extent of forest structure tested (90 x 90m). Resilience of these forests is likely compromised by structural
37 homogenization from a century of fire suppression, but could be restored with management that increases
38 forest structural variability.

39 **Introduction**

40 Forests are essential components of the biosphere, and ensuring their persistence is of high management
41 priority given their large carbon stores and other valued ecosystem services (Trumbore *et al.* 2015; Higuera
42 *et al.* 2019). Modern forests are subject to disturbances that are increasingly frequent, intense, and entangled
43 with human society, which may compromise their resilience and their ability to persist (Millar & Stephenson
44 2015; Seidl *et al.* 2016; Schoennagel *et al.* 2017; Hessburg *et al.* 2019; McWethy *et al.* 2019). A resilient
45 forest can absorb disturbances and may reorganize, but is unlikely to transition to an alternate vegetation
46 type in the long run (Holling 1973; Walker *et al.* 2004). Resilience can arise when interactions amongst
47 heterogeneous elements within a system create stabilizing negative feedbacks, or interrupt positive feedbacks
48 that would otherwise cause critical transitions (Peters *et al.* 2004; Reyer *et al.* 2015a). System resilience
49 can be generated by heterogeneity at a variety of organizational scales, including genetic diversity (Reusch
50 *et al.* 2005), species diversity (Chesson 2000), functional diversity (Gazol & Camarero 2016), topoclimatic
51 complexity (Lenoir *et al.* 2013), and temporal environmental variation (Questad & Foster 2008). Forest
52 resilience mechanisms are fundamentally difficult to quantify because forests comprise long-lived species, span
53 large geographic extents, and are affected by disturbances at a broad range of spatial scales (Reyer *et al.*
54 2015a, b). It is therefore critical, but challenging, to understand the system-wide mechanisms underlying
55 forest resilience and the extent to which humans have the capacity to influence them.

56 Wildfire severity describes a fire’s effect on vegetation (Keeley 2009) and high-severity fire, in which all or
57 nearly all overstory vegetation is killed, can be a precursor to state transitions in dry coniferous forests

58 (Stevens *et al.* 2017; Davis *et al.* 2019). For several centuries prior to Euroamerican invasion, fire regimes
59 in this ecosystem were variable as a consequence of both natural and Indigenous burning, with primarily
60 low- and moderate-severity fire and localized patches of high-severity fire (Safford & Stevens 2017). Most
61 dry coniferous tree species in frequent-fire forests did not evolve mechanisms to protect propagules (e.g.,
62 seeds, buds/stems that can resprout) from high-severity fire, so recruitment in large patches with few or no
63 surviving trees is often limited by longer-distance dispersal of tree seeds from unburned or lower-severity
64 areas (Welch *et al.* 2016; Stevens-Rumann & Morgan 2019). In the Sierra Nevada, the absence of tree seeds
65 after severe wildfire can lead to forest regeneration failure as resprouting shrubs outcompete slower-growing
66 conifer seedlings and provide continuous cover of flammable fuel that makes future high-severity wildfire more
67 likely (Collins & Roller 2013; Coppoletta *et al.* 2016), though this pathway doesn't materialize in forests with
68 a slower postfire vegetation response (Prichard & Kennedy 2014; Stevens-Rumann *et al.* 2016). Dry forest
69 regeneration is especially imperiled after high-severity fire when postfire climate conditions are suboptimal
70 for conifer seedling establishment (Davis *et al.* 2019) or optimal for shrub regeneration (Young *et al.* 2019).
71 Many dry western U.S. forests are experiencing "unhealthy" conditions which leaves them prone to catastrophic
72 shifts in ecosystem type (Millar & Stephenson 2015; McWethy *et al.* 2019). First, a century of fire suppression
73 has drastically increased forest density and fuel connectivity (Safford & Stevens 2017), which increases
74 competition for water (D'Amato *et al.* 2013; van Mantgem *et al.* 2016) and favors modern wildfires with
75 large, contiguous patches of tree mortality whose interiors are far from potential seed sources (Miller & Thode
76 2007; Safford & Stevens 2017; Stevens *et al.* 2017; Steel *et al.* 2018). Second, warmer temperatures coupled
77 with recurrent drought exacerbate water stress on trees (Williams *et al.* 2013; Millar & Stephenson 2015;
78 Clark *et al.* 2016), producing conditions favorable for high-intensity fire (Fried *et al.* 2004; Abatzoglou &
79 Williams 2016) and less suitable for postfire conifer establishment (Stevens-Rumann *et al.* 2018; Davis *et al.*
80 2019). Thus, the presence of stabilizing feedbacks that limit high-severity fire may represent a fundamental
81 resilience mechanism of dry coniferous forests, but anthropogenic climate and management impacts may be
82 upsetting those feedbacks and eroding forest resilience.

83 Resilience to disturbances such as wildfire may derive from heterogeneity in vegetation structure (Turner &
84 Romme 1994; Stephens *et al.* 2008; North *et al.* 2009; Virah-Sawmy *et al.* 2009). Forest structure— the size
85 and spatial distribution of vegetation in a forest— links past and future fire disturbance via feedbacks with fire
86 behavior (Agee 1996). A structurally variable forest with horizontally and vertically discontinuous fuel may
87 experience slower-moving surface fires, a lower probability of crown fire initiation and spread, and a reduced
88 potential for self-propagating, eruptive behavior (Scott & Reinhardt 2001; Graham *et al.* 2004; Peters *et al.*
89 2004; Fox & Whitesides 2015; Parsons *et al.* 2017). Feeding back to influence forest structure, this milder fire

90 behavior, characteristic of pre-Euroamerican settlement conditions in dry western U.S. forests, generates a
91 heterogeneous patchwork of fire effects including consumed understory vegetation, occasional overstory tree
92 mortality, and highly variable structure at a fine scale (Sugihara *et al.* 2006; Scholl & Taylor 2010; Cansler &
93 McKenzie 2014; Safford & Stevens 2017). Thus, more structurally variable dry forests are often considered
94 more resilient and are predicted to persist in the face of frequent wildfire disturbance (Graham *et al.* 2004;
95 Moritz *et al.* 2005; Stephens *et al.* 2008).

96 While the homogenizing effect of modern high-severity fire on forest structure is well-documented (Steel *et*
97 *al.* 2018), the foundational concept of feedback between heterogeneity of forest structure and fire severity is
98 underexplored at the ecosystem scale, in part because of the dual challenges of measuring fine-grain vegetation
99 heterogeneity at broad spatial extents (Kane *et al.* 2015; Graham *et al.* 2019) and linking local, bottom-up
100 processes to emergent ecosystem-wide patterns in an empirical setting (Turner & Romme 1994; Bessie &
101 Johnson 1995; McKenzie & Kennedy 2011, 2012). Furthermore, it has been difficult to resolve the “scale of
102 effect” (Graham *et al.* 2019) for how variability in forest structure is meaningful for resilience (Kotliar &
103 Wiens 1990; Turner *et al.* 2013).

104 Advances in the accessibility and tractability of spatiotemporally extensive Earth observation data (Gorelick
105 *et al.* 2017) provide an avenue to insight into fundamental ecosystem properties at relevant scales, such as
106 resilience mechanisms of vast, long-lived forests. We use Landsat satellite imagery and a massively-parallel
107 image processing approach to calculate wildfire severity for over 1,000 Sierra Nevada yellow pine/mixed-conifer
108 wildfires encompassing a wide size range (4 to >100,000 hectares) and long time series (1984 to 2018). We
109 calibrate these spectral severity measures to ground assessments of fire effects on overstory trees from 208
110 field plots. For each point within these ~1,000 fires, we use texture analysis (Haralick *et al.* 1973) at multiple
111 scales to characterize local variability in vegetation structure across broad spatial extents and determine
112 its “scale of effect” (Graham *et al.* 2019). We pair the resulting extensive database of wildfire severity and
113 multiple scales of local forest variability to ask: (1) Does spatial variability in forest structure increase the
114 resilience of California yellow pine/mixed-conifer forests by reducing the severity of wildfires? (2) What is
115 the “scale of effect” of structural variability that influences wildfire severity? and (3) Does the influence of
116 structural variability on fire severity depend on topography, regional climate, or other conditions?

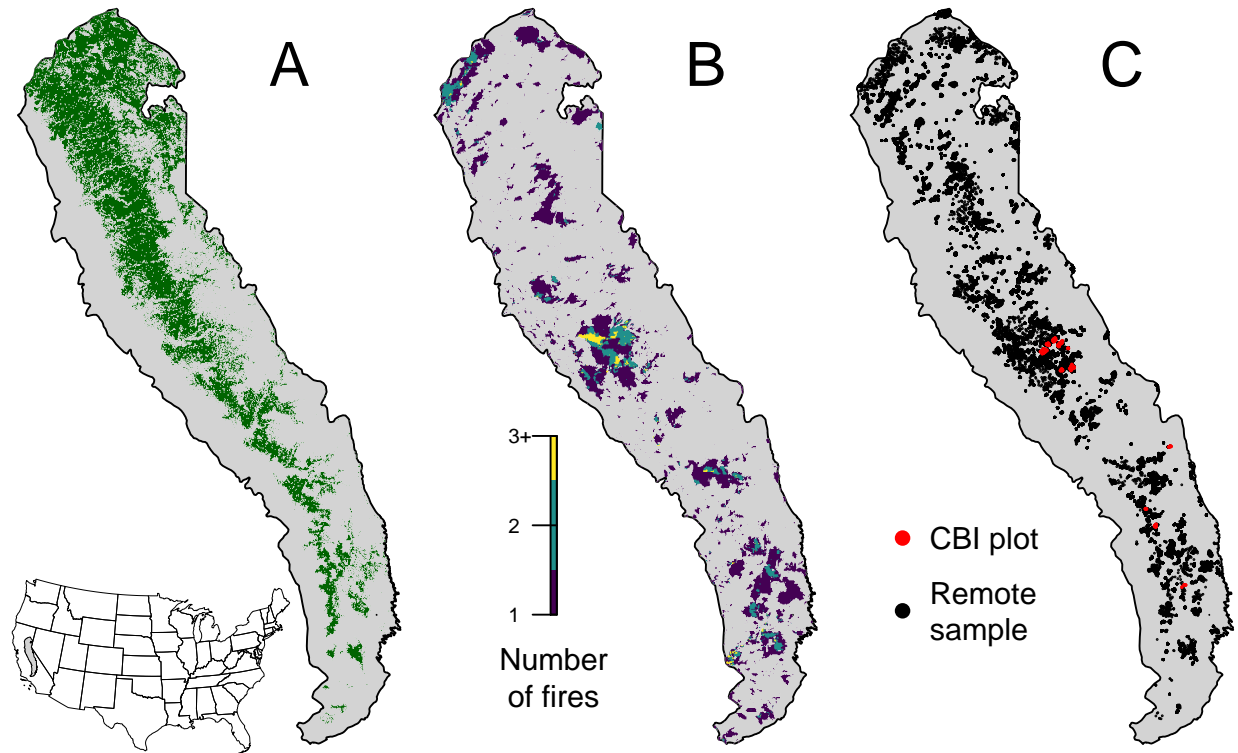


Fig. 1. Geographic setting of the study. A) Location of yellow pine/mixed-conifer forests as designated by the Fire Return Interval Departure (FRID) product which, among other things, describes the potential vegetation in an area based on the pre-Euroamerican settlement fire regime. B) Locations of all fires covering greater than 4 hectares that burned in yellow pine/mixed-conifer forest between 1984 and 2018 in the Sierra Nevada mountain range of California according to the State of California Fire Resource and Assessment Program database, the most comprehensive database of fire perimeters of its kind. Colors indicate how many fire perimeters overlapped a given pixel within the study time period. C) (red) Locations of 208 composite burn index (CBI) ground plots used to calibrate the remotely sensed measures of severity. (black) Locations of random samples drawn from 1008 unique fires depicted in panel B that were in yellow pine/mixed-conifer forest as depicted in panel A, and which were designated as “burned” by exceeding a threshold relative burn ratio (RBR) determined by calibrating the algorithm presented in this study with ground-based CBI measurements.

117 **Material and Methods**

118 **Study system**

119 Our study assesses the effect of vegetation structure on wildfire severity in the Sierra Nevada mountain range
120 of California in yellow pine/mixed-conifer forests (Fig. 1; Supp. methods). This system is dominated by
121 a mixture of conifer species including ponderosa pine (*Pinus ponderosa*), sugar pine (*Pinus lambertiana*),
122 incense-cedar (*Calocedrus decurrens*), Douglas-fir (*Pseudotsuga menziesii*), white fir (*Abies concolor*), and red
123 fir (*Abies magnifica*), angiosperm trees primarily including black oak (*Quercus kelloggii*), as well as shrubs
124 (*Ceanothus* spp., *Arctostaphylos* spp.) (Safford & Stevens 2017).

125 **Programatically assessing wildfire severity**

126 We measured forest vegetation characteristics and wildfire severity using imagery from the Landsat series of
127 satellites post-processed to surface reflectance using radiometric corrections (Masek *et al.* 2006; Vermote *et*
128 *al.* 2016; USGS 2017b, a). Landsat satellites image the entire Earth approximately every 16 days with a 30m
129 pixel resolution. We used Google Earth Engine for image collation and processing (Gorelick *et al.* 2017).

130 We calculated wildfire severity for the most comprehensive record of fire perimeters in California: the Fire
131 and Resource Assessment Program (FRAP) fire perimeter database ([https://frap.fire.ca.gov/frap-projects/
132 fire-perimeters/](https://frap.fire.ca.gov/frap-projects/fire-perimeters/)). The FRAP database includes all known fires that covered more than 4 hectares, compared
133 to the regional standard database which includes fires covering greater than 80 hectares (Miller & Safford
134 2012; Steel *et al.* 2018) and the national standard database Monitoring Trends in Burn Severity (MTBS)
135 which includes fires covering greater than 400 hectares in the western U.S. (Eidenshink *et al.* 2007). Smaller
136 fire events are important contributors to fire regimes, but their effects are often underrepresented in analyses
137 of fire effects (Randerson *et al.* 2012). The FRAP perimeters are error-checked, but it is possible that
138 duplicated events are occasionally represented in the database. Using the FRAP database, we quantified fire
139 severity within each perimeter of 1008 wildfires in the Sierra Nevada yellow pine/mixed-conifer forest that
140 burned between 1984 and 2018, which more than doubles the number of fire events with severity assessments
141 compared to the regional standard database.

142 We created per-pixel median composites of collections of pre- and postfire images for each fire to calculate
143 common spectral indices of wildfire severity. Prefire image collections spanned a fixed time window ending
144 the day before each fire’s discovery date and postfire image collections spanned the same fixed time window,
145 exactly one year after the prefire window. We tested four different time periods (16, 32, 48, and 64 days) that
146 defined the time window of the pre- and postfire image collections, and seven common spectral indices of

147 severity (RBR, dNBR, RdNBR, dNBR2, RdNBR2, dNDVI, RdNDVI) for a total of 28 different means to
148 remotely measure wildfire severity (Supp. methods).

149 We calibrated these 28 severity metrics with 208 field assessments of fire effects from previous studies (Zhu *et*
150 *al.* 2006; Sikkink *et al.* 2013). Severity was measured in the field as the overstory component of the Composite
151 Burn Index (CBI)—a metric of vegetation mortality across several vertical vegetation strata within a 30m
152 diameter field plot. The overstory component of CBI characterizes fire effects to the overstory vegetation
153 specifically, which includes both dominant/co-dominant big trees as well as intermediate-sized subcanopy
154 trees (generally 10-25 cm DBH and 8-20m tall) (Key & Benson 2006). CBI ranges from 0 (no fire impacts) to
155 3 (very high fire impacts), and is a common standard for calibrating remotely-sensed severity data in western
156 U.S. forests (Key & Benson 2006; Miller & Thode 2007; Miller *et al.* 2009; Cansler & McKenzie 2012; Parks
157 *et al.* 2014, 2018; Prichard & Kennedy 2014). We extracted each spectral severity metric at the CBI plot
158 locations using both bilinear and bicubic interpolation (Cansler & McKenzie 2012; Parks *et al.* 2014, 2018)
159 and fit a non-linear model:

$$160 \quad (1) \text{ remote_severity} = \beta_0 + \beta_1 e^{\beta_2 \text{cbi_overstory}}$$

161 We treated the spectral severity measure as the dependent variable in this nonlinear regression for comparison
162 with other studies (Miller & Thode 2007; Miller *et al.* 2009; Parks *et al.* 2014). We performed ten-fold cross
163 validation using the `modelr` and `purrr` packages (Henry & Wickham 2019; Wickham 2019) and report the
164 average R^2 value for each model. We used the severity calculation derived from the best fitting model for all
165 further analyses (Relative Burn Ratio [RBR] calculated using a 48-day time window; ten-fold cross validation
166 $R^2 = 0.806$; first panel of Fig. 2; Supp. Table 1).

167 Using the non-linear relationship between RBR and CBI, we calculated the threshold RBR corresponding to
168 “high-severity” signifying complete or near-complete overstory mortality using the common CBI high-severity
169 lower threshold of 2.25 (i.e., an RBR value of 282.335; Fig. 3) (Miller & Thode 2007).

170 **Assessing local forest structure variability at broad extents**

171 We used texture analysis to calculate a remotely-sensed measure of local forest variability (Haralick *et al.*
172 1973; Tuanmu & Jetz 2015). Within a moving square neighborhood window with sides of 90m (3x3 pixels),
173 150m (5x5 pixels), 210m (7x7 pixels), and 270m (9x9 pixels), we calculated forest variability for each pixel as
174 the standard deviation of the NDVI values of its neighbors (not including itself). NDVI correlates well with
175 foliar biomass, leaf area index, and vegetation cover (Rouse *et al.* 1973), so a higher standard deviation of
176 NDVI within a given local neighborhood corresponds to discontinuous canopy cover and abrupt vegetation

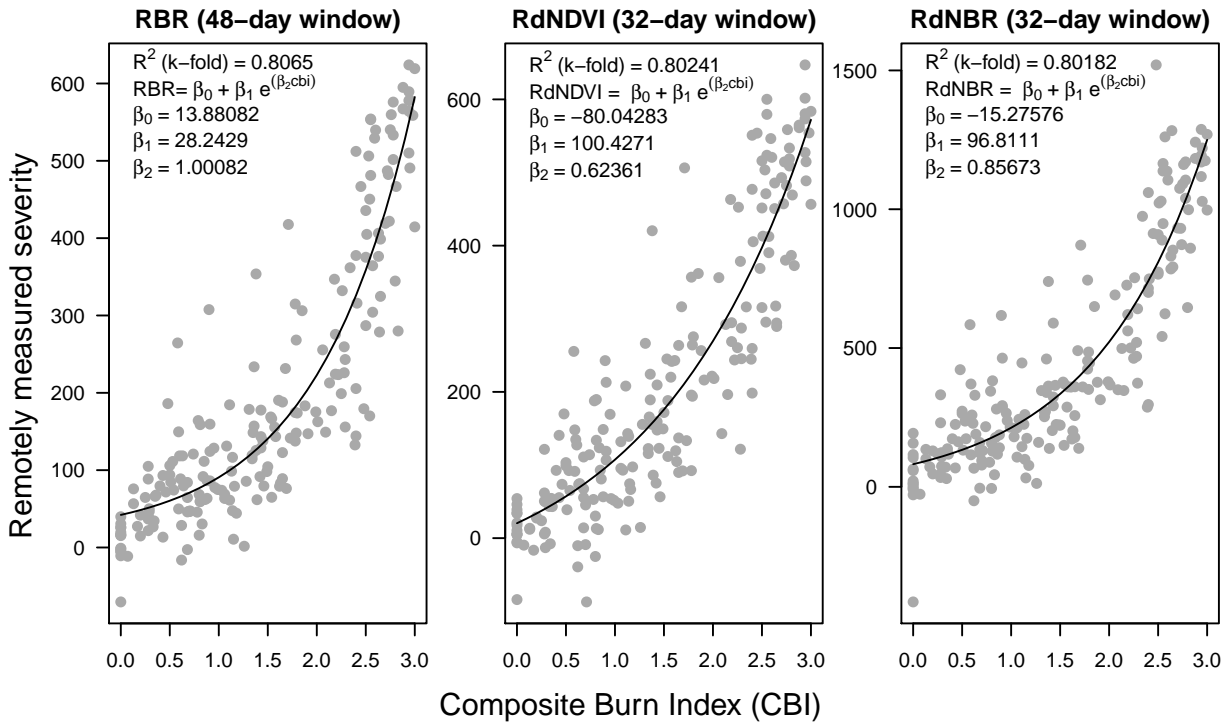


Fig. 2. Three top performing remotely-sensed severity metrics based on ten-fold cross validation (relative burn ratio, 48-day window, bicubic interpolation; relative delta normalized burn ratio, 32-day window, bilinear interpolation; and relative delta normalized difference vegetation index, 48-day window, bilinear interpolation) calculated using new automated image collation algorithms, calibrated to 208 field measures of fire severity (composite burn index). See Supplemental Table 1 for performance of all tested models.

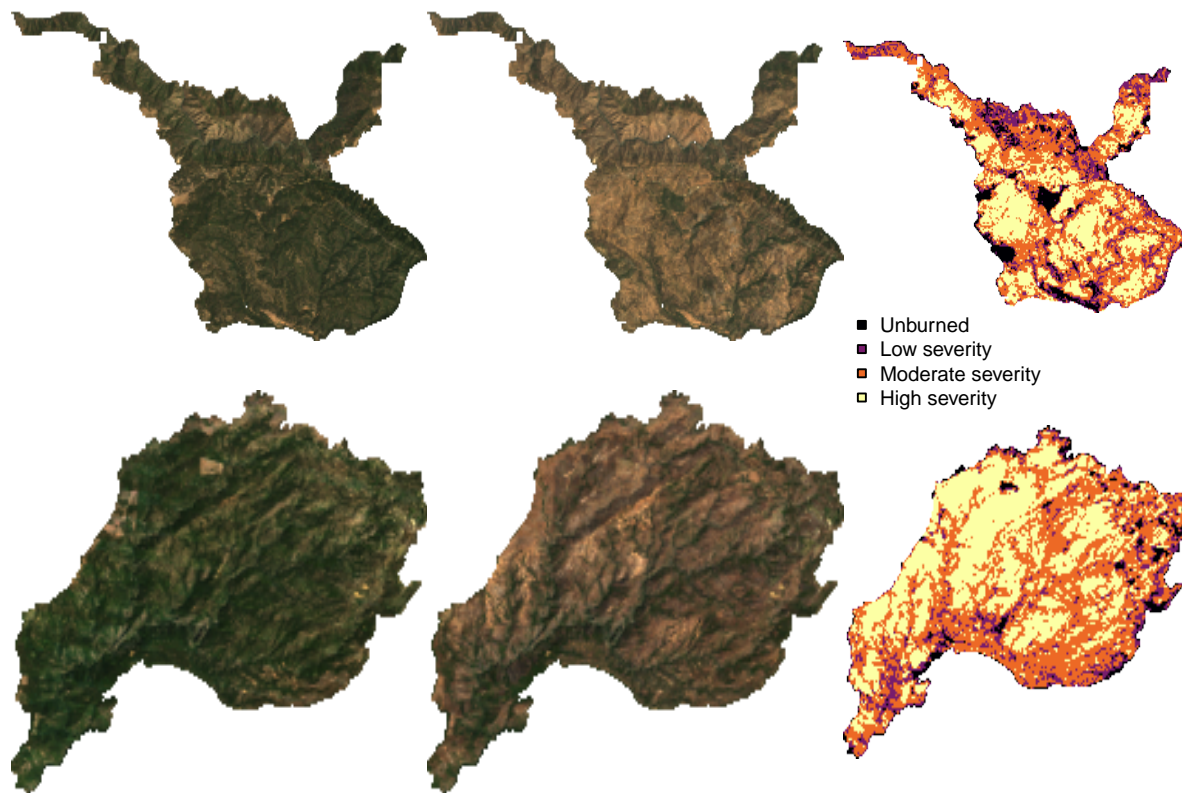


Fig. 3. Example algorithm outputs for the Hamm Fire of 1987 (top half) and the American Fire of 2013 (bottom half) showing: prefire true color composite image (left third), postfire true color composite image (center third), relative burn ratio (RBR) calculation using a 48-day image collation window before the fire and one year later (right third). For visualization purposes, these algorithm outputs have been resampled to a resolution of 100m x 100m from their original resolution of 30 x 30m, and the continuous severity index has been binned into severity categories. Data used for analyses were sampled from the outputs at the original resolution.

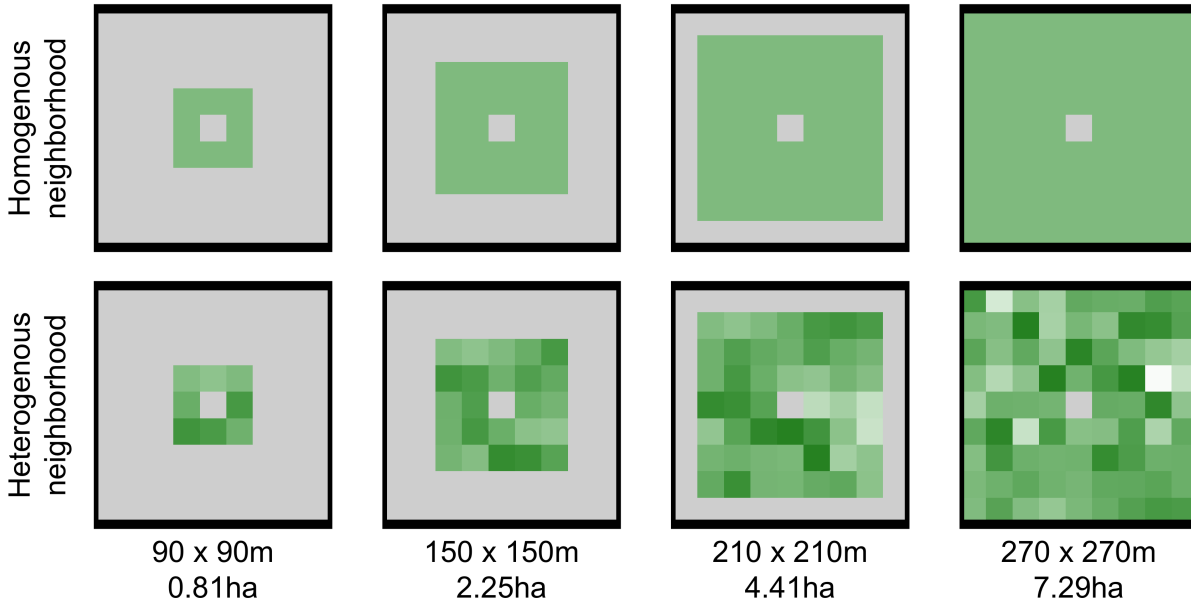


Fig. 4. Example of homogenous forest (top row) and heterogenous forest (bottom row) with the same mean NDVI values (~ 0.6). Each column represents forest structural variability measured using a different neighborhood size. NDVI is represented by a white to green color gradient, and pixels that are not included in the forest structural variability metric are colored gray.

177 edges (see Fig. 4) (Franklin *et al.* 1986).

178 Assessing other conditions

179 Elevation data were sourced from a 1-arc second digital elevation model (DEM) (Farr *et al.* 2007) which was
 180 used to calculate slope, aspect, and potential annual heat load— an integrated measure of latitude, slope, and
 181 aspect (McCune & Keon (2002); Supp. methods). Per-pixel topographic roughness was calculated as the
 182 standard deviation of elevation values within the same-sized kernels as those used for variability in forest
 183 structure (90m, 150m, 210m, and 270m on a side and not including the central pixel). We chose this specific
 184 measure of topographic roughness because it directly parallels and accounts for our metric of forest structure
 185 variability and because of its use in other studies (Holden *et al.* 2009), though other measures of topographic
 186 heterogeneity have been used for fire modeling (Haire & McGarigal 2009; Holden *et al.* 2009; Cansler &
 187 McKenzie 2014).

188 We calculated prefire fuel moisture as the median 100-hour fuel moisture for the 3 days prior to the fire
 189 using gridMET, a gridded meteorological product with a daily temporal resolution and a 4km x 4km spatial
 190 resolution (Abatzoglou 2013). The 100-hour fuel moisture is a correlate of the regional temperature and
 191 moisture which integrates the relative humidity, the length of day, and the amount of precipitation in the

192 previous 24 hours. Thus, this measure is sensitive to multiple hot dry days across the 4km x 4km spatial
193 extent of each grid cell, but not to diurnal variation in relative humidity nor to extreme weather events during
194 a fire.

195 **Modeling**

196 Approximately 100 random points were selected within each FRAP fire perimeter in areas designated as
197 yellow pine/mixed-conifer forest and we extracted the values of severity and covariate at those points using
198 nearest neighbor interpolation. Using the calibration equation described in Eq. 1 for the best configuration
199 of the remote severity metric, we removed sampled points corresponding to “unburned” area prior to analysis
200 (i.e., below an RBR threshold of 45.097). The random sampling amounted to 56088 total samples across 1008
201 fires.

202 We used a hierarchical logistic regression model (Eq. 2) to assess the probability of high-severity wildfire as a
203 linear combination of the remote metrics described above: prefire NDVI of each pixel, standard deviation of
204 NDVI within a neighborhood (i.e., forest structural variability), the mean NDVI within a neighborhood, 100-
205 hour fuel moisture, potential annual heat load, and topographic roughness. We included two-way interactions
206 between the structural variability measure and prefire NDVI, neighborhood mean NDVI, and 100-hour fuel
207 moisture. We include the two-way interaction between a pixel’s prefire NDVI and its neighborhood mean
208 NDVI to account for structural variability that may arise from contrasts between these variables (e.g., “holes
209 in the forest” vs. “isolated patches”; Supp. Fig. 2). We scaled all predictor variables, used weakly-regularizing
210 priors, and estimated an intercept for each individual fire with pooled variance (i.e., a group-level effect of
211 fire). We used the `brms` package to fit models in a Bayesian framework which implements the No U-Turn
212 Sampler extension to the Hamiltonian Monte Carlo algorithm (Hoffman & Gelman 2014; Bürkner 2017). We
213 used 4 chains with 5000 samples per chain (including 2500 warmup samples) and chain convergence was
214 assessed for each estimated parameter by ensuring Rhat values were less than or equal to 1.01 (Bürkner 2017).

$$severity_{i,j} \sim Bern(\phi_{i,j})$$

$$\beta_0 +$$

$$\beta_{nbhd_stdev_NDVI} * nbhd_stdev_NDVI_i +$$

$$\beta_{prefire_NDVI} * prefire_NDVI_i +$$

$$\beta_{nbhd_mean_NDVI} * nbhd_mean_NDVI_i +$$

$$\beta_{fm100} * fm100_i +$$

$$215 \quad (2) \quad logit(\phi_{i,j}) = \beta_{pahl} * pahl_i +$$

$$\beta_{topographic_roughness} * topographic_roughness_i +$$

$$\beta_{nbhd_stdev_NDVI*fm100} * nbhd_stdev_NDVI_i * fm100_i +$$

$$\beta_{nbhd_stdev_NDVI*prefire_NDVI} * nbhd_stdev_NDVI_i * prefire_NDVI_i +$$

$$\beta_{nbhd_stdev_NDVI*nbhd_mean_NDVI} * nbhd_stdev_NDVI_i * nbhd_mean_NDVI_i +$$

$$\beta_{nbhd_mean_NDVI*prefire_NDVI} * nbhd_mean_NDVI_i * prefire_NDVI_i +$$

$$\gamma_j$$

$$\gamma_j \sim \mathcal{N}(0, \sigma_{fire})$$

216 Scale of effect of forest structure variability

217 Each neighborhood size (90m, 150m, 210m, 270m) was substituted in turn for the neighborhood standard
 218 deviation of NDVI, neighborhood mean NDVI, and terrain roughness covariates to generate a candidate set
 219 of 4 models. To assess the scale at which these neighborhood-size-dependent effects manifested, we compared
 220 the 4 candidate models using leave-one-out cross validation (Vehtari *et al.* 2017). We inferred that the
 221 neighborhood size window used in the best-performing model reflected the scale at which the forest structure
 222 variability effect had the most support (Graham *et al.* 2019). We used R for all statistical analyses (R Core
 223 Team 2018).

224 Results

225 Our programmatic assessment of wildfire severity calibrates as well or better than other reported methods
 226 that often require substantial manual intervention (Edwards *et al.* 2018). We found that this approach was
 227 robust to a wide range of spectral severity metrics, time windows, and interpolation techniques, including
 228 those based on NDVI are seldom-used in this system (Fig. 2; Supp. Tab. 1; Supp. methods).

Tab. 1: Comparison of four models described in Eq. 2 using different neighborhood sizes for calculating forest structural variability (standard deviation of NDVI within the neighborhood), neighborhood mean NDVI, and topographic roughness (standard deviation of elevation within the neighborhood). LOO is a measure of a model’s predictive accuracy (with lower values corresponding to more accurate prediction) and is calculated as -2 times the expected log pointwise predictive density (elpd) for a new dataset (Vehtari *et al.* 2017). Δ LOO is the difference between a model’s LOO and the lowest LOO in a set of models (i.e., the model with the best predictive accuracy). The Bayesian R^2 is a ‘data-based estimate of the proportion of variance explained for new data’ (Gelman *et al.* 2018). Note that Bayesian R^2 values are conditional on the model so shouldn’t be compared across models, though they can be informative about a single model at a time.

Model	Neighborhood size					
	for variability measure	LOO (-2*elpd)	Δ LOO to best model	SE of Δ LOO	LOO model weight (%)	Bayesian R^2
1	90 x 90m	42364	0	NA	100	0.300
2	150 x 150m	42417	53.17	14.99	0	0.299
3	210 x 210m	42459	94.44	21.35	0	0.299
4	270 x 270m	42491	126.5	25.15	0	0.298

229 The model with the best out-of-sample prediction accuracy assessed by leave-one-out cross validation was
 230 the model fit using the smallest neighborhood size for the variability of forest structure (standard deviation
 231 of neighborhood NDVI), the mean of neighborhood NDVI, and the terrain roughness (standard deviation
 232 of elevation) (Tab. 1). One hundred percent of the model weight belongs to the model using the smallest
 233 neighborhood size window.

234 We report the results from fitting the model described in Eq. 2 using the smallest neighborhood size (90
 235 x 90m) because this was the best performing model (see above) and because the size and magnitude of
 236 estimated coefficients were similar across neighborhood sizes (Supp. Tab. 2).

237 The strongest influence on the probability of a forested area burning at high-severity was the a pixel’s prefire
 238 NDVI, with a greater prefire NDVI increasing the probability of high-severity fire ($\beta_{\text{prefire_ndvi}} = 1.06$; 95%
 239 CI: [0.931, 1.192]); Fig. 5). There was a strong negative relationship between 100-hour fuel moisture and
 240 wildfire severity such that increasing 100-hour fuel moisture was associated with a decreasing probability
 241 of a high-severity wildfire ($\beta_{\text{fm100}} = -0.576$; 95% CI: [-0.709, -0.442]) (Fig. 5). Potential annual heat load,
 242 which integrates aspect, slope, and latitude, also had a strong positive relationship with the probability of
 243 a high-severity fire. Areas that were located on southwest facing sloped terrain at lower latitudes had the
 244 highest potential annual heat load, and were more likely to burn at high-severity ($\beta_{\text{pahl}} = 0.246$; 95% CI:
 245 [0.215, 0.277]) Fig. 5). We found a negative effect of the prefire neighborhood mean NDVI on the probability

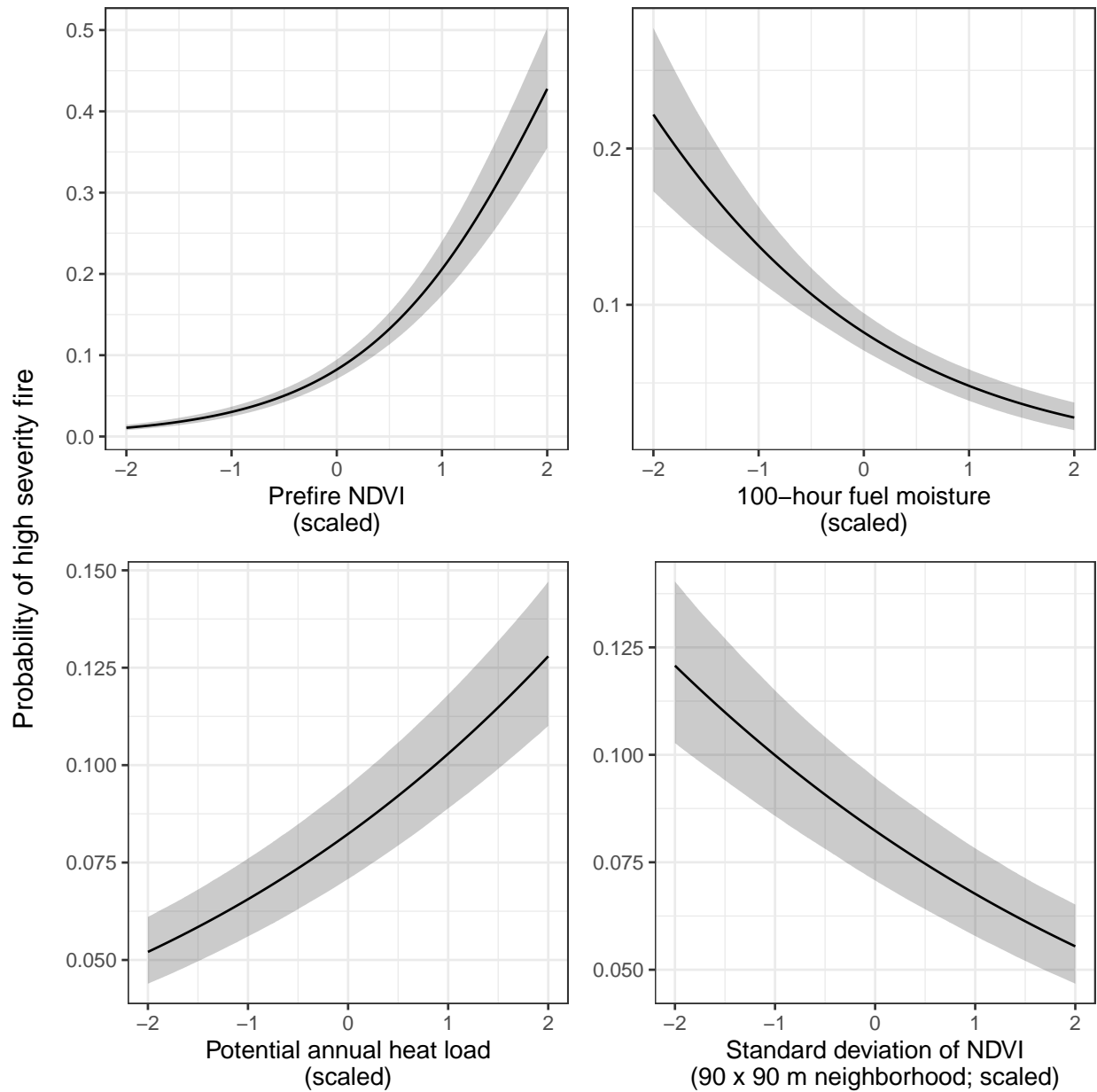


Fig. 5. The main effects and 95% credible intervals of the covariates having the strongest relationships with the probability of high-severity fire. All depicted relationships derive from the model using the 90m x 90m neighborhood size window for neighborhood standard deviation of NDVI, neighborhood mean of NDVI, and topographic roughness, as this was the best performing model of the four neighborhood sizes tested. The effect sizes of these covariates were similar for each neighborhood size tested.

246 of a pixel burning at high-severity ($\beta_{\text{nbhd_mean_NDVI}} = -0.168$; 95% CI: [-0.311, -0.028]). This is in contrast
247 to the positive effect of the prefire NDVI of the pixel itself. We found no effect of local topographic roughness
248 on wildfire severity ($\beta_{\text{topographic_roughness}} = 0.002$; 95% CI: [-0.029, 0.034]).

249 There was also a strong negative interaction between the neighborhood mean NDVI and the prefire NDVI of
250 the central pixel ($\beta_{\text{nbhd_mean_NDVI*prefire_NDVI}} = -0.54$; 95% CI: [-0.587, -0.494]).

251 From the same model, we found strong evidence for a negative effect of variability of vegetation structure
252 on the probability of a high-severity wildfire ($\beta_{\text{nbhd_stdev_NDVI}} = -0.213$; 95% CI: [-0.251, -0.174]); Fig. 5).

253 We also found significant interactions between variability of vegetation structure and prefire NDVI of the
254 central pixel ($\beta_{\text{nbhd_stdev_NDVI*prefire_NDVI}} = 0.128$; 95% CI: [0.031, 0.221]) as well as between variability of
255 vegetation structure and neighborhood mean NDVI ($\beta_{\text{nbhd_stdev_NDVI*nbhd_mean_NDVI}} = -0.115$; 95% CI:
256 [-0.206, -0.022]).

257 Discussion

258 Broad-extent, fine-grain, spatially-explicit analyses of whole ecosystems are key to illuminating macroecological
259 phenomena such as forest resilience to disturbance (Heffernan *et al.* 2014). We used a powerful, cloud-based
260 geographic information system and data repository, Google Earth Engine, as a ‘macroscope’ (Beck *et al.*
261 2012) to study feedbacks between vegetation structure and wildfire disturbance in yellow pine/mixed-conifer
262 forests of California’s Sierra Nevada mountain range. With this approach, we reveal and quantify general
263 features of this forest system, and gain deeper insights into the mechanisms underlying its function.

264 High-severity wildfire and ecological resilience

265 Wildfire severity can be considered a direct correlate of a forest’s resistance– the ease or difficulty with which
266 a disturbance changes the system state (Folke *et al.* 2004; Walker *et al.* 2004). One relevant state change for
267 assessing ecosystem resistance is the loss of its characteristic native biota (Keith *et al.* 2013), which could be
268 represented as overstory tree mortality (e.g., severity) in a forested system. The same fire behavior in two
269 different forest systems (e.g., old-growth conifer versus young conifer plantation) may have very different
270 abilities to cause overstory mortality (Keeley 2009), which reflects differences in each forest’s resistance.
271 Resistance is a key component of resilience (Folke *et al.* 2004; Walker *et al.* 2004) and, in this framework,
272 one manifestation of forest resilience is high resistance to wildfire, whereby some mechanism leads to lower
273 severity when a fire occurs. Here, we show clear evidence that structural heterogeneity fulfills this mechanistic
274 resistance role in dry coniferous systems (Fig. 5). This study thus provides a particularly extensive, large-scale

275 example of an association between local structural heterogeneity and ecosystem resilience, a phenomenon
276 that has been demonstrated in other systems at smaller scales.

277 These findings do not imply that resistance to fire is a sole or necessary path to resilience. For instance, high-
278 severity fire is characteristic of other forest systems such as serotinous lodgepole pine forests in Yellowstone
279 National Park, and is not ordinarily expected to hamper forest regeneration (Turner *et al.* 1997). Our inference
280 that structural variability is a fundamental resilience mechanism in dry coniferous forests is strengthened by
281 its large effect size and our ability to measure the negative feedback phenomenon at relevant spatiotemporal
282 scales: we captured local-scale variability in structure and wildfire severity at broad spatial extents for an
283 extensive set of over 1,000 fires across a 34-year time span.

284 **Factors influencing the probability of high-severity wildfire**

285 We found that the strongest influence on the probability of high-severity wildfire was prefire NDVI. Greater
286 NDVI corresponds to high canopy cover and vegetation density (Rouse *et al.* 1973) which translates directly
287 to live fuel loads in the forest canopy and can increase high-severity fire (Parks *et al.* 2018). Overstory canopy
288 cover and density also correlate (though weakly) with surface fuel loads (Lydersen *et al.* 2015; Collins *et*
289 *al.* 2016; Cansler *et al.* 2019), which can play a large role in driving high-severity fire in these forests (Agee
290 1996). Thus NDVI is likely a strong predictor of fire severity because it is correlated with both surface fuel
291 loads and canopy live fuel density.

292 We found a strong positive effect of potential annual heat load as well as a strong negative effect of 100-hour
293 fuel moisture, results which corroborates similar studies (Parks *et al.* 2018). Some work has shown that
294 terrain roughness (Haire & McGarigal 2009; Holden *et al.* 2009; Dillon *et al.* 2011; Krawchuk *et al.* 2016)
295 can be an important predictor of wildfire severity, but we found no effect using our measure of local terrain
296 variability. This may be a function of scale—our measures of topographic roughness were more localized than
297 those of other studies (Holden *et al.* 2009; Dillon *et al.* 2011). Haire & McGarigal (2009) also found occasional
298 instances where small differences in topographic roughness had dramatic differences in severity. These sorts
299 of influences on severity would be challenging to detect in our modeling framework, which was designed to
300 estimate an overall influence of topographic roughness on fire severity. Also, topographic roughness could
301 be measured in different ways that highlight different types of heterogeneity (Haralick *et al.* 1973), which
302 suggests that an effect of topographic roughness on mean wildfire severity will be best-captured by a roughness
303 measure that aligns with the dominant phenomenon driving that effect. Finally, the observed influence of
304 topographic roughness in other studies may have been fully or partially driven by variability in vegetation,
305 which we partition separately in our study.

306 Critically, we found a strong negative effect of forest structural variability on wildfire severity that was
307 opposite in direction but similar in magnitude to the effect of potential annual heat load. Just as the positive
308 effect of NDVI is likely driven by increased fuel loads, the negative effect of variability in NDVI, is likely
309 driven by discontinuity in surface, ladder, and canopy fuels, which can reduce the probability of initiation
310 and spread of tree-killing crown fires (Wagner 1977; Agee 1996; Graham *et al.* 2004). This discontinuity can
311 manifest in a number of ways. For instance, neighboring forest pixels with different tree size distributions
312 may disrupt a crown fire's spread from a low to a high crown or vice versa. Local NDVI variability may also
313 reflect heterogeneous arrangement of vegetation types such as a forested pixel adjacent to a pixel mostly
314 covered by grass. In the grass-dominated area, the relatively low flame heights would likely fail to initiate or
315 sustain active crowning behavior that would kill overstory trees in the neighboring forested area. Finally,
316 forest structural variability may also arise with different land cover types in the local neighborhood that
317 influence severity, such as when exposed bedrock or a group of boulders acts as fire refugia for vegetation
318 rooted within it (Hylander & Johnson 2010).

319 **Feedback between forest structural variability and wildfire severity**

320 This system-wide inverse relationship between structural variability and wildfire severity closes a feedback
321 that links past and future fire behavior via forest structure. Frequent wildfire in dry coniferous forests
322 generates variable forest structure (North *et al.* 2009; Larson & Churchill 2012; Malone *et al.* 2018), which in
323 turn, as we demonstrate, dampens the severity of future fire. In contrast, exclusion of wildfire homogenizes
324 forest structure and increases the probability that a fire will produce large, contiguous patches of overstory
325 mortality (Stevens *et al.* 2017; Steel *et al.* 2018). The proportion and spatial configuration of fire severity in
326 fire-prone forests are key determinants of their long-term persistence (Stevens *et al.* 2017; Steel *et al.* 2018).
327 Lower-severity fire or scattered patches of higher-severity fire reduce the risk of conversion to a non-forest
328 vegetation type (Kemp *et al.* 2016; Stevens-Rumann *et al.* 2018; Walker *et al.* 2018), while prospects for
329 forest regeneration are bleaker when high-severity patch sizes are much larger than the natural range of
330 variation for the system (Miller & Safford 2017; Stevens *et al.* 2017; Stevens-Rumann & Morgan 2019). Thus,
331 the forest-structure-mediated feedback between past and future fire severity underlies the resilience of the
332 Sierra Nevada yellow pine/mixed-conifer system.

333 **Scale of effect of variability in forest structure**

334 We found that the effect of a forest patch's neighborhood characteristics on the probability of high-severity fire
335 was strongest at the smallest neighborhood size that we tested, 90 x 90m. This suggests that the moderating

336 effect of forest structure variability on fire severity is a very local phenomenon. This corroborates work by
337 Safford *et al.* (2012), who found that crown fires (high tree-killing potential) were almost always reduced to
338 surface fires (low tree-killing potential) within 70m of entering a fuel reduction treatment area.

339 Severity patterns at a landscape scale (e.g., for a whole fire) may represent cross-scale emergences of the local
340 influence of forest structure variability on fire effects (Peters *et al.* 2004; Rose *et al.* 2017). For instance,
341 forest management actions (e.g., prescribed fire, use of wildfire under mild conditions) that reduce fuel loads
342 and increase structural variability can be effective at reducing fire severity across broader spatial extents
343 than the direct footprints of those actions (Graham *et al.* 2004; Stephens *et al.* 2009; Tubbesing *et al.* 2019).
344 Some work suggests that this sort of cross-scale emergence may depend on even broader-scale effects of fire
345 weather, with small-scale variability failing to influence fire behavior under extreme conditions (Peters *et al.*
346 2004; Lydersen *et al.* 2014), though we did not detect such an interaction between our metric of burning
347 conditions (100-hour fuel moisture) and forest structure variability.

348 **Correlation between covariates and interactions**

349 Unexpectedly, we found a strong interaction between the prefire NDVI at a pixel and its neighborhood mean
350 NDVI on the probability of high-severity fire. These two variables are strongly correlated (Spearman’s $\rho =$
351 0.97), so the general effect of this interaction is to dampen the dominating effect of prefire NDVI. Thus,
352 though the marginal effect of prefire NDVI on the probability of high-severity fire is still positive and large,
353 its real-world effect might be more comparable to other modeled covariates when including the negative main
354 effect of neighborhood mean NDVI, the negative interaction effect of prefire NDVI and neighborhood mean
355 NDVI, and their tendency to covary (compare the effect of prefire NDVI under the common scenario of prefire
356 NDVI and neighborhood mean NDVI increasing or decreasing together: $\beta_{\text{prefire_ndvi}} + \beta_{\text{nbhd_mean_NDVI}} +$
357 $\beta_{\text{nbhd_mean_NDVI}*\text{prefire_NDVI}} = 0.352$, to the effect of 100-hour fuel moisture, which becomes the effect with
358 the greatest magnitude: $\beta_{\text{fm100}} = -0.576$).

359 In the few cases when prefire NDVI and the neighborhood mean NDVI contrast, there is an overall effect
360 of increasing the probability of high-severity fire. When prefire NDVI at the central pixel is high and the
361 neighborhood NDVI is low (e.g., an isolated vegetation patch; Supplemental Fig. 2), the probability of
362 high-severity fire is expected to dramatically increase. When prefire NDVI at the central pixel is low and the
363 neighborhood NDVI is high (e.g., a hole in the forest; Supp. Fig. 2), the probability of high-severity fire at
364 that central pixel is still expected to be fairly high even though vegetation is sparse there. In these forest
365 NDVI datasets, when these variables do decouple, they tend to do so in the “hole in the forest” case and lead
366 to a greater probability of high-severity fire at the central pixel despite its low NDVI. This can perhaps be

367 explained if the consistently high vegetation density in a local neighborhood– itself more likely to burn at
368 high-severity– exerts a contagious effect on the central pixel, raising its probability of burning at high-severity
369 regardless of how much fuel might be there to burn.

370 **Conclusions**

371 Theory and empirical work suggest a general link between forest structural heterogeneity and resilience. Here
372 we find strong evidence with a large-scale study that, across large areas of forest, variable forest structure
373 generally makes yellow pine/mixed-conifer forest in the Sierra Nevada more resistant to inevitable wildfire
374 disturbance. It has been well-documented that frequent, low-severity wildfire maintains forest structural
375 variability. Here, we demonstrate a system-wide reciprocal effect suggesting that greater local-scale variability
376 of vegetation structure makes fire-prone, dry forests more resilient to wildfire and may increase the probability
377 of their long-term persistence.

378 **Acknowledgements**

379 We thank Connie Millar, Derek Young, and Meagan Oldfather for valuable comments about this work and
380 we also thank the community of Google Earth Engine developers for prompt and helpful insights about the
381 platform. We thank four anonymous reviewers for their helpful comments on the manuscript. Funding for
382 this work was provided by NSF Graduate Research Fellowship Grant #DGE- 1321845 Amend. 3 as well as
383 by Earth Lab through CU Boulder’s Grand Challenge Initiative and the Cooperative Institute for Research
384 in Environmental Sciences (CIRES) at CU Boulder (to MJK).

385 **References**

- 386 1.
387 Abatzoglou, J.T. (2013). Development of gridded surface meteorological data for ecological applications and
388 modelling. *International Journal of Climatology*, 33, 121–131.
- 389 2.
390 Abatzoglou, J.T. & Williams, A.P. (2016). Impact of anthropogenic climate change on wildfire across western
391 U.S. Forests. *Proceedings of the National Academy of Sciences*, 113, 11770–11775.
- 392 3.
393 Agee, J.K. (1996). The influence of forest structure on fire behavior. *17th Forest Vegetation Management*

- 394 *Conference*, 17.
- 395 4.
- 396 Beck, J., Ballesteros-Mejia, L., Buchmann, C.M., Dengler, J., Fritz, S.A. & Gruber, B. *et al.* (2012). What's
397 on the horizon for macroecology? *Ecography*, 35, 673–683.
- 398 5.
- 399 Bessie, W.C. & Johnson, E.A. (1995). The relative importance of fuels and weather on fire behavior in
400 subalpine forests. *Ecology*, 76, 747–762.
- 401 6.
- 402 Bürkner, P.-C. (2017). **brms**: An *R* package for bayesian multilevel models using *Stan*. *Journal of Statistical*
403 *Software*, 80.
- 404 7.
- 405 Cansler, C.A. & McKenzie, D. (2012). How robust are burn severity indices when applied in a new region?
406 Evaluation of alternate field-based and remote-sensing methods. *Remote Sensing*, 4, 456–483.
- 407 8.
- 408 Cansler, C.A. & McKenzie, D. (2014). Climate, fire size, and biophysical setting control fire severity and
409 spatial pattern in the northern Cascade Range, USA. *Ecological Applications*, 24, 1037–1056.
- 410 9.
- 411 Cansler, C.A., Swanson, M.E., Furniss, T.J., Larson, A.J. & Lutz, J.A. (2019). Fuel dynamics after
412 reintroduced fire in an old-growth Sierra Nevada mixed-conifer forest. *Fire Ecology*, 15, 16.
- 413 10.
- 414 Chesson, P. (2000). Mechanisms of maintenance of species diversity. *Annual Review of Ecology and Systematics*,
415 31, 343–366.
- 416 11.
- 417 Clark, J.S., Iverson, L., Woodall, C.W., Allen, C.D., Bell, D.M. & Bragg, D.C. *et al.* (2016). The impacts
418 of increasing drought on forest dynamics, structure, and biodiversity in the United States. *Global Change*
419 *Biology*, 22, 2329–2352.
- 420 12.
- 421 Collins, B.M., Lydersen, J.M., Fry, D.L., Wilkin, K., Moody, T. & Stephens, S.L. (2016). Variability in
422 vegetation and surface fuels across mixed-conifer-dominated landscapes with over 40 years of natural fire.
423 *Forest Ecology and Management*, 381, 74–83.

424 13.

425 Collins, B.M. & Roller, G.B. (2013). Early forest dynamics in stand-replacing fire patches in the northern
426 Sierra Nevada, California, USA. *Landscape Ecology*, 28, 1801–1813.

427 14.

428 Coppoletta, M., Merriam, K.E. & Collins, B.M. (2016). Post-fire vegetation and fuel development influences
429 fire severity patterns in reburns. *Ecological Applications*, 26, 686–699.

430 15.

431 D’Amato, A.W., Bradford, J.B., Fraver, S. & Palik, B.J. (2013). Effects of thinning on drought vulnerability
432 and climate response in north temperate forest ecosystems. *Ecological Applications*, 23, 1735–1742.

433 16.

434 Davis, K.T., Dobrowski, S.Z., Higuera, P.E., Holden, Z.A., Veblen, T.T. & Rother, M.T. *et al.* (2019).
435 Wildfires and climate change push low-elevation forests across a critical climate threshold for tree regeneration.
436 *PNAS*, 201815107.

437 17.

438 Dillon, G.K., Holden, Z.A., Morgan, P., Crimmins, M.A., Heyerdahl, E.K. & Luce, C.H. (2011). Both
439 topography and climate affected forest and woodland burn severity in two regions of the western U.S., 1984
440 to 2006. *Ecosphere*, 2, art130.

441 18.

442 Edwards, A.C., Russell-Smith, J. & Maier, S.W. (2018). A comparison and validation of satellite-derived fire
443 severity mapping techniques in fire prone north Australian savannas: Extreme fires and tree stem mortality.
444 *Remote Sensing of Environment*, 206, 287–299.

445 19.

446 Eidenshink, J., Schwind, B., Brewer, K., Zhu, Z.-L., Quayle, B. & Howard, S. (2007). A project for monitoring
447 trends in burn severity. *Fire Ecology*, 3, 3–21.

448 20.

449 Farr, T.G., Rosen, P.A., Caro, E., Crippen, R., Duren, R. & Hensley, S. *et al.* (2007). The shuttle radar
450 topography mission. *Reviews of Geophysics*, 45.

451 21.

452 Folke, C., Carpenter, S., Walker, B., Scheffer, M., Elmqvist, T. & Gunderson, L. *et al.* (2004). Regime shifts,
453 resilience, and biodiversity in ecosystem management. *Annual Review of Ecology, Evolution, and Systematics*,

454 3, 557–581.

455 22.

456 Fox, J.M. & Whitesides, G.M. (2015). Warning signals for eruptive events in spreading fires. *Proceedings of*
457 *the National Academy of Sciences*, 112, 2378–2383.

458 23.

459 Franklin, J., Logan, T., Woodcock, C. & Strahler, A. (1986). Coniferous forest classification and inventory
460 using Landsat and digital terrain data. *IEEE Transactions on Geoscience and Remote Sensing*, GE-24,
461 139–149.

462 24.

463 Fried, J.S., Torn, M.S. & Mills, E. (2004). The impact of climate change on wildfire severity: A regional
464 forecast for Northern California. *Climatic Change*, 64, 169–191.

465 25.

466 Gazol, A. & Camarero, J.J. (2016). Functional diversity enhances silver fir growth resilience to an extreme
467 drought. *Journal of Ecology*, 104, 1063–1075.

468 26.

469 Gelman, A., Goodrich, B., Gabry, J. & Vehtari, A. (2018). R-squared for Bayesian regression models. *The*
470 *American Statistician*, 1–6.

471 27.

472 Gorelick, N., Hancher, M., Dixon, M., Ilyushchenko, S., Thau, D. & Moore, R. (2017). Google Earth Engine:
473 Planetary-scale geospatial analysis for everyone. *Remote Sensing of Environment*, 202, 18–27.

474 28.

475 Graham, L.J., Spake, R., Gillings, S., Watts, K. & Eigenbrod, F. (2019). Incorporating fine-scale environmental
476 heterogeneity into broad-extent models. *Methods in Ecology and Evolution*, 10, 767–778.

477 29.

478 Graham, R.T., McCaffrey, S. & Jain, T.B. (2004). *Science basis for changing forest structure to modify*
479 *wildfire behavior and severity* (No. RMRS-GTR-120). U.S. Department of Agriculture, Forest Service, Rocky
480 Mountain Research Station, Ft. Collins, CO.

481 30.

482 Haire, S.L. & McGarigal, K. (2009). Changes in fire severity across gradients of climate, fire size, and
483 topography: A landscape ecological perspective. *fire ecol*, 5, 86–103.

484 31.

485 Haralick, R.M., Shanmugam, K. & Dinstein, I. (1973). Textural features for image classification. *IEEE*
486 *Transactions on Systems, Man, and Cybernetics*, SMC-3, 610–621.

487 32.

488 Heffernan, J.B., Soranno, P.A., Angilletta, M.J., Buckley, L.B., Gruner, D.S. & Keitt, T.H. *et al.* (2014).
489 Macrosystems ecology: Understanding ecological patterns and processes at continental scales. *Frontiers in*
490 *Ecology and the Environment*, 12, 5–14.

491 33.

492 Henry, L. & Wickham, H. (2019). *Purrr: Functional programming tools*.

493 34.

494 Hessburg, P.F., Miller, C.L., Povak, N.A., Taylor, A.H., Higuera, P.E. & Prichard, S.J. *et al.* (2019). Climate,
495 environment, and disturbance history govern resilience of western North American forests. *Front. Ecol. Evol.*,
496 7.

497 35.

498 Higuera, P.E., Metcalf, A.L., Miller, C., Buma, B., McWethy, D.B. & Metcalf, E.C. *et al.* (2019). Integrating
499 subjective and objective dimensions of resilience in fire-prone landscapes. *BioScience*, 69, 379–388.

500 36.

501 Hoffman, M.D. & Gelman, A. (2014). The No-U-Turn Sampler: Adaptively setting path lengths in Hamiltonian
502 Monte Carlo. *Journal of Machine Learning Research*, 15, 31.

503 37.

504 Holden, Z.A., Morgan, P. & Evans, J.S. (2009). A predictive model of burn severity based on 20-year satellite-
505 inferred burn severity data in a large southwestern US wilderness area. *Forest Ecology and Management*, 258,
506 2399–2406.

507 38.

508 Holling, C.S. (1973). Resilience and stability of ecological systems. *Annual Review of Ecology and Systematics*,
509 1–23.

510 39.

511 Hylander, K. & Johnson, S. (2010). In situ survival of forest bryophytes in small-scale refugia after an intense
512 forest fire. *Journal of Vegetation Science*, 21, 1099–1109.

513 40.

514 Kane, V.R., Cansler, C.A., Povak, N.A., Kane, J.T., McGaughey, R.J. & Lutz, J.A. *et al.* (2015). Mixed
515 severity fire effects within the Rim fire: Relative importance of local climate, fire weather, topography, and
516 forest structure. *Forest Ecology and Management*, 358, 62–79.

517 41.

518 Keeley, J.E. (2009). Fire intensity, fire severity and burn severity: A brief review and suggested usage.
519 *International Journal of Wildland Fire*, 18, 116.

520 42.

521 Keith, D.A., Rodríguez, J.P., Rodríguez-Clark, K.M., Nicholson, E., Aapala, K. & Alonso, A. *et al.* (2013).
522 Scientific foundations for an IUCN red list of ecosystems. *PLoS ONE*, 8, e62111.

523 43.

524 Kemp, K.B., Higuera, P.E. & Morgan, P. (2016). Fire legacies impact conifer regeneration across environmental
525 gradients in the U.S. Northern Rockies. *Landscape Ecol*, 31, 619–636.

526 44.

527 Key, C.H. & Benson, N.C. (2006). Landscape assessment (LA): Sampling and analysis methods, 55.

528 45.

529 Kotliar, N.B. & Wiens, J.A. (1990). Multiple scales of patchiness and patch structure: A hierarchical
530 framework for the study of heterogeneity. *Oikos*, 59, 253.

531 46.

532 Krawchuk, M.A., Haire, S.L., Coop, J., Parisien, M.-A., Whitman, E. & Chong, G. *et al.* (2016). Topographic
533 and fire weather controls of fire refugia in forested ecosystems of northwestern North America. *Ecosphere*, 7,
534 e01632.

535 47.

536 Larson, A.J. & Churchill, D. (2012). Tree spatial patterns in fire-frequent forests of western North America,
537 including mechanisms of pattern formation and implications for designing fuel reduction and restoration
538 treatments. *Forest Ecology and Management*, 267, 74–92.

539 48.

540 Lenoir, J., Graae, B.J., Aarrestad, P.A., Alsos, I.G., Armbruster, W.S. & Austrheim, G. *et al.* (2013). Local
541 temperatures inferred from plant communities suggest strong spatial buffering of climate warming across
542 Northern Europe. *Global Change Biology*, 19, 1470–1481.

543 49.

544 Lydersen, J.M., Collins, B.M., Knapp, E.E., Roller, G.B. & Stephens, S. (2015). Relating fuel loads to
545 overstorey structure and composition in a fire-excluded Sierra Nevada mixed conifer forest. *International*
546 *Journal of Wildland Fire*, 24, 484.

547 50.

548 Lydersen, J.M., North, M.P. & Collins, B.M. (2014). Severity of an uncharacteristically large wildfire, the
549 Rim Fire, in forests with relatively restored frequent fire regimes. *Forest Ecology and Management*, 328,
550 326–334.

551 51.

552 Malone, S., Fornwalt, P., Battaglia, M., Chambers, M., Iniguez, J. & Sieg, C. (2018). Mixed-severity fire
553 fosters heterogeneous spatial patterns of conifer regeneration in a dry conifer forest. *Forests*, 9, 45.

554 52.

555 van Mantgem, P.J., Caprio, A.C., Stevenson, N.L. & Das, A.J. (2016). Does prescribed fire promote resistance
556 to drought in low elevation forests of the Sierra Nevada, California, USA? *Fire Ecology*, 12, 13–25.

557 53.

558 Masek, J., Vermote, E., Saleous, N., Wolfe, R., Hall, F. & Huemmrich, K. *et al.* (2006). A Landsat surface
559 reflectance dataset for North America, 1990–2000. *IEEE Geoscience and Remote Sensing Letters*, 3, 68–72.

560 54.

561 McCune, B. & Keon, D. (2002). Equations for potential annual direct incident radiation and heat load.
562 *Journal of Vegetation Science*, 13, 603–606.

563 55.

564 McKenzie, D. & Kennedy, M.C. (2011). Scaling laws and complexity in fire regimes. In: *The Landscape*
565 *Ecology of Fire* (eds. McKenzie, D., Miller, C. & Falk, D.A.). Springer Netherlands, Dordrecht, pp. 27–49.

566 56.

567 McKenzie, D. & Kennedy, M.C. (2012). Power laws reveal phase transitions in landscape controls of fire
568 regimes. *Nature Communications*, 3, 726.

569 57.

570 McWethy, D.B., Schoennagel, T., Higuera, P.E., Krawchuk, M., Harvey, B.J. & Metcalf, E.C. *et al.* (2019).
571 Rethinking resilience to wildfire. *Nat Sustain*, 1–8.

572 58.

573 Millar, C.I. & Stephenson, N.L. (2015). Temperate forest health in an era of emerging megadisturbance.

574 *Science*, 349, 823–826.

575 59.

576 Miller, J.D., Knapp, E.E., Key, C.H., Skinner, C.N., Isbell, C.J. & Creasy, R.M. *et al.* (2009). Calibration and
577 validation of the relative differenced Normalized Burn Ratio (RdNBR) to three measures of fire severity in
578 the Sierra Nevada and Klamath Mountains, California, USA. *Remote Sensing of Environment*, 113, 645–656.

579 60.

580 Miller, J.D. & Safford, H. (2012). Trends in wildfire severity: 1984 to 2010 in the Sierra Nevada, Modoc
581 Plateau, and Southern Cascades, California, U.S.A. *Fire Ecology*, 8, 41–57.

582 61.

583 Miller, J.D. & Safford, H.D. (2017). Corroborating evidence of a pre-Euro-American low- to moderate-severity
584 fire regime in yellow pineMixed conifer forests of the Sierra Nevada, California, USA. *Fire Ecology*, 13, 58–90.

585 62.

586 Miller, J.D. & Thode, A.E. (2007). Quantifying burn severity in a heterogeneous landscape with a relative
587 version of the delta Normalized Burn Ratio (dNBR). *Remote Sensing of Environment*, 109, 66–80.

588 63.

589 Moritz, M.A., Morais, M.E., Summerell, L.A., Carlson, J.M. & Doyle, J. (2005). Wildfires, complexity, and
590 highly optimized tolerance. *Proceedings of the National Academy of Sciences*, 102, 17912–17917.

591 64.

592 North, M., Stine, P., O’Hara, K., Zielinski, W. & Stephens, S. (2009). *An ecosystem management strategy for*
593 *Sierran mixed-conifer forests* (No. PSW-GTR-220). U.S. Department of Agriculture, Forest Service, Pacific
594 Southwest Research Station, Albany, CA.

595 65.

596 Parks, S.A., Holsinger, L.M., Panunto, M.H., Jolly, W.M., Dobrowski, S.Z. & Dillon, G.K. (2018). High-
597 severity fire: Evaluating its key drivers and mapping its probability across western U.S. Forests. *Environmental*
598 *Research Letters*, 13, 044037.

599 66.

600 Parks, S., Dillon, G. & Miller, C. (2014). A new metric for quantifying burn severity: The Relativized Burn
601 Ratio. *Remote Sensing*, 6, 1827–1844.

602 67.

603 Parsons, R.A., Linn, R.R., Pimont, F., Hoffman, C., Sauer, J. & Winterkamp, J. *et al.* (2017). Numerical

604 investigation of aggregated fuel spatial pattern impacts on fire behavior. *Land*, 6, 43.
605 68.
606 Peters, D.P.C., Pielke, R.A., Bestelmeyer, B.T., Allen, C.D., Munson-McGee, S. & Havstad, K.M. (2004).
607 Cross-scale interactions, nonlinearities, and forecasting catastrophic events. *Proceedings of the National*
608 *Academy of Sciences*, 101, 15130–15135.
609 69.
610 Prichard, S.J. & Kennedy, M.C. (2014). Fuel treatments and landform modify landscape patterns of burn
611 severity in an extreme fire event. *Ecological Applications*, 24, 571–590.
612 70.
613 Questad, E.J. & Foster, B.L. (2008). Coexistence through spatio-temporal heterogeneity and species sorting
614 in grassland plant communities. *Ecology Letters*, 11, 717–726.
615 71.
616 Randerson, J.T., Chen, Y., Werf, G.R. van der, Rogers, B.M. & Morton, D.C. (2012). Global burned area
617 and biomass burning emissions from small fires. *Journal of Geophysical Research: Biogeosciences*, 117.
618 72.
619 R Core Team. (2018). *R: A language and environment for statistical computing*. R Foundation for Statistical
620 Computing, Vienna, Austria.
621 73.
622 Reusch, T.B.H., Ehlers, A., Hammerli, A. & Worm, B. (2005). Ecosystem recovery after climatic extremes
623 enhanced by genotypic diversity. *Proceedings of the National Academy of Sciences*, 102, 2826–2831.
624 74.
625 Reyer, C.P.O., Brouwers, N., Rammig, A., Brook, B.W., Epila, J. & Grant, R.F. *et al.* (2015a). Forest
626 resilience and tipping points at different spatio-temporal scales: Approaches and challenges. *Journal of*
627 *Ecology*, 103, 5–15.
628 75.
629 Reyer, C.P., Rammig, A., Brouwers, N. & Langerwisch, F. (2015b). Forest resilience, tipping points and
630 global change processes. *Journal of Ecology*, 103, 1–4.
631 76.
632 Rose, K.C., Graves, R.A., Hansen, W.D., Harvey, B.J., Qiu, J. & Wood, S.A. *et al.* (2017). Historical
633 foundations and future directions in macrosystems ecology. *Ecology Letters*, 20, 147–157.

634 77.

635 Rouse, W., Haas, R.H., Deering, W. & Schell, J.A. (1973). *Monitoring the vernal advancement and*
636 *retrogradation (green wave effect) of natural vegetation* (Type II Report No. RSC 1978-2). Goddard Space
637 Flight Center, Greenbelt, MD, USA.

638 78.

639 Safford, H.D. & Stevens, J.T. (2017). *Natural range of variation for yellow pine and mixed-conifer forests*
640 *in the Sierra Nevada, Southern Cascades, and Modoc and Inyo National Forests, California, USA* (No.
641 PSW-GTR-256).

642 79.

643 Safford, H., Stevens, J., Merriam, K., Meyer, M. & Latimer, A. (2012). Fuel treatment effectiveness in
644 California yellow pine and mixed conifer forests. *Forest Ecology and Management*, 274, 17–28.

645 80.

646 Schoennagel, T., Balch, J.K., Brenkert-Smith, H., Dennison, P.E., Harvey, B.J. & Krawchuk, M.A. *et al.*
647 (2017). Adapt to more wildfire in western North American forests as climate changes. *Proceedings of the*
648 *National Academy of Sciences*, 114, 4582–4590.

649 81.

650 Scholl, A.E. & Taylor, A.H. (2010). Fire regimes, forest change, and self-organization in an old-growth
651 mixed-conifer forest, Yosemite National Park, USA. *Ecological Applications*, 20, 362–380.

652 82.

653 Scott, J.H. & Reinhardt, E.D. (2001). *Assessing crown fire potential by linking models of surface and crown*
654 *fire behavior* (No. RMRS-RP-29). U.S. Department of Agriculture, Forest Service, Rocky Mountain Research
655 Station, Ft. Collins, CO.

656 83.

657 Seidl, R., Spies, T.A., Peterson, D.L., Stephens, S.L. & Hicke, J.A. (2016). Searching for resilience: Addressing
658 the impacts of changing disturbance regimes on forest ecosystem services. *J Appl Ecol*, 53, 120–129.

659 84.

660 Sikkink, P.G., Dillon, G.K., Keane, R.E., Morgan, P., Karau, E.C. & Holden, Z.A. *et al.* (2013). Composite
661 Burn Index (CBI) data and field photos collected for the FIRESEV project, western United States.

662 85.

663 Steel, Z.L., Koontz, M.J. & Safford, H.D. (2018). The changing landscape of wildfire: Burn pattern trends

664 and implications for California's yellow pine and mixed conifer forests. *Landscape Ecology*, 33, 1159–1176.

665 86.

666 Stephens, S.L., Fry, D.L. & Franco-Vizcaíno, E. (2008). Wildfire and spatial patterns in forests in Northwestern
667 Mexico: The United States wishes it had similar fire problems. *Ecology and Society*, 13.

668 87.

669 Stephens, S.L., Moghaddas, J.J., Edminster, C., Fiedler, C.E., Haase, S. & Harrington, M. *et al.* (2009). Fire
670 treatment effects on vegetation structure, fuels, and potential fire severity in western U.S. Forests. *Ecological*
671 *Applications*, 19, 305–320.

672 88.

673 Stevens, J.T., Collins, B.M., Miller, J.D., North, M.P. & Stephens, S.L. (2017). Changing spatial patterns of
674 stand-replacing fire in California conifer forests. *Forest Ecology and Management*, 406, 28–36.

675 89.

676 Stevens-Rumann, C.S., Kemp, K.B., Higuera, P.E., Harvey, B.J., Rother, M.T. & Donato, D.C. *et al.* (2018).
677 Evidence for declining forest resilience to wildfires under climate change. *Ecology Letters*, 21, 243–252.

678 90.

679 Stevens-Rumann, C.S. & Morgan, P. (2019). Tree regeneration following wildfires in the western US: A
680 review. *fire ecol*, 15, 15.

681 91.

682 Stevens-Rumann, C.S., Prichard, S.J., Strand, E.K. & Morgan, P. (2016). Prior wildfires influence burn
683 severity of subsequent large fires. *Canadian Journal of Forest Research*, 46, 1375–1385.

684 92.

685 Sugihara, N.G., Wagtendonk, J.W.V., Fites-Kaufman, J., Shaffer, K.E. & Thode, A.E. (2006). *Fire in*
686 *California's Ecosystems*. University of California Press.

687 93.

688 Trumbore, S., Brando, P. & Hartmann, H. (2015). Forest health and global change. *Science*, 349, 814–818.

689 94.

690 Tuanmu, M.-N. & Jetz, W. (2015). A global, remote sensing-based characterization of terrestrial habitat
691 heterogeneity for biodiversity and ecosystem modelling: Global habitat heterogeneity. *Global Ecology and*
692 *Biogeography*, 24, 1329–1339.

693 95.

694 Tubbesing, C.L., Fry, D.L., Roller, G.B., Collins, B.M., Fedorova, V.A. & Stephens, S.L. *et al.* (2019).
695 Strategically placed landscape fuel treatments decrease fire severity and promote recovery in the northern
696 Sierra Nevada. *Forest Ecology and Management*, 436, 45–55.

697 96.

698 Turner, M.G., Donato, D.C. & Romme, W.H. (2013). Consequences of spatial heterogeneity for ecosystem
699 services in changing forest landscapes: Priorities for future research. *Landscape Ecology*, 28, 1081–1097.

700 97.

701 Turner, M.G. & Romme, W.H. (1994). Landscape dynamics in crown fire ecosystems. *Landscape Ecol*, 9,
702 59–77.

703 98.

704 Turner, M.G., Romme, W.H., Gardner, R.H. & Hargrove, W.W. (1997). Effects of fire size and pattern on
705 early succession in Yellowstone National Park. *Ecological Monographs*, 67, 411.

706 99.

707 USGS. (2017a). Landsat 4-7 Surface Reflectance (LEDAPS) Product Guide, 41.

708 100.

709 USGS. (2017b). Landsat 8 Surface Reflectance Code (LASRC) Product Guide, 40.

710 101.

711 Vehtari, A., Gelman, A. & Gabry, J. (2017). Practical Bayesian model evaluation using leave-one-out
712 cross-validation and WAIC. *Statistics and Computing*, 27, 1413–1432.

713 102.

714 Vermote, E., Justice, C., Claverie, M. & Franch, B. (2016). Preliminary analysis of the performance of the
715 Landsat 8/OLI land surface reflectance product. *Remote Sensing of Environment*, 185, 46–56.

716 103.

717 Virah-Sawmy, M., Gillson, L. & Willis, K.J. (2009). How does spatial heterogeneity influence resilience to
718 climatic changes? Ecological dynamics in southeast Madagascar. *Ecological Monographs*, 79, 557–574.

719 104.

720 Wagner, C.E.V. (1977). Conditions for the start and spread of crown fire. *Can. J. For. Res.*, 7, 23–34.

721 105.

722 Walker, B., Holling, C.S., Carpenter, S.R. & Kinzig, A.P. (2004). Resilience, adaptability, and transformability
723 in social-ecological systems. *Ecology and Society*, 9.

724 106.

725 Walker, R.B., Coop, J.D., Parks, S.A. & Trader, L. (2018). Fire regimes approaching historic norms reduce
726 wildfire-facilitated conversion from forest to non-forest. *Ecosphere*, 9, e02182.

727 107.

728 Welch, K.R., Safford, H.D. & Young, T.P. (2016). Predicting conifer establishment post wildfire in mixed
729 conifer forests of the North American Mediterranean-climate zone. *Ecosphere*, 7, e01609.

730 108.

731 Wickham, H. (2019). *Modelr: Modelling functions that work with the pipe*.

732 109.

733 Williams, A.P., Allen, C.D., Macalady, A.K., Griffin, D., Woodhouse, C.A. & Meko, D.M. *et al.* (2013).
734 Temperature as a potent driver of regional forest drought stress and tree mortality. *Nature Climate Change*,
735 3, 292–297.

736 110.

737 Young, D.J.N., Werner, C.M., Welch, K.R., Young, T.P., Safford, H.D. & Latimer, A.M. (2019). Post-fire
738 forest regeneration shows limited climate tracking and potential for drought-induced type conversion. *Ecology*,
739 100, e02571.

740 111.

741 Zhu, Z., Key, C., Ohlen, D. & Benson, N. (2006). *Evaluate sensitivities of burn-severity mapping algorithms*
742 *for different ecosystems and fire histories in the United States* (Final Report to the Joint Fire Science Program
743 No. JFSP 01-1-4-12).